

See discussions, stats, and author profiles for this publication at: <https://www.researchgate.net/publication/231371045>

# Corrosive Behavior of Tungsten in Post Dry-Etch Residue Remover

ARTICLE *in* INDUSTRIAL & ENGINEERING CHEMISTRY RESEARCH · SEPTEMBER 2003

Impact Factor: 2.59 · DOI: 10.1021/ie030025h

---

CITATIONS

7

---

READS

135

5 AUTHORS, INCLUDING:



Bing-Hung Chen

National Cheng Kung University

91 PUBLICATIONS 1,661 CITATIONS

SEE PROFILE

# Corrosive Behavior of Tungsten in Post Dry-Etch Residue Remover

Bing-Hung Chen,<sup>\*,†</sup> Hao Zhang,<sup>‡,§</sup> Simon Y.M. Chooi,<sup>§</sup> Lap Chan,<sup>§</sup> Y. Xu,<sup>⊥</sup> and J. H. Ye<sup>⊥</sup>

Department of Chemical Engineering, National Cheng Kung University, 1 University Road, Tainan 70101, Taiwan, Department of Chemical and Environmental Engineering, National University of Singapore, 10 Kent Ridge Crescent, Singapore 119260, Department of Technology Development, Chartered Semiconductor Manufacturing Ltd., 60 Woodland Industrial Park D, Street 2, Singapore 738406, and Institute of Materials Research and Engineering, 3 Research Link, Singapore 117602

Failure of the tungsten (W) plug has become the main reliability issue in post-metal-etch cleaning due to the interaction between tungsten and the alkanolamine or hydroxylamine ingredients in the cleaning solution, as well as tungsten and chloride from the previous chlorine-based etching process. In our efforts to understand tungsten plug corrosion, the electrochemical behavior of blanket tungsten films in the post-etch resist remover, the EKC265 solution, at 65 °C in the presence of deionized water and  $\text{Cl}^-$  was investigated using Tafel extrapolation, potentiometry, X-ray photoelectron spectroscopy (XPS), and scanning electron microscopy (SEM). The corrosion-current density and the open-circuit potential data showed that the basic EKC265 solution was aggressive to tungsten. The addition of chloride ions ( $\text{Cl}^-$ ) and the deionized water to the EKC265 solution further increased the corrosion-current density and shifted the open-circuit potential to more negative values. SEM pictures gave visual evidence of changes on the tungsten surface due to corrosion. Pitting was observed in the presence of both deionized water and  $\text{Cl}^-$ . The changes in the chemical composition of tungsten films were evaluated with XPS. It was found that the distribution of oxidation states of tungsten was largely influenced by the chemical treatment in the EKC265-based electrolytes and closely related to the corrosion resistance of tungsten in the electrolytes.

## 1. Introduction

Miniaturization of device features on an integrated circuit, including isolation, gates, storage nodes, interconnects, and metallization, is essential for advanced device technologies. The tungsten plug is one of the device features which links the first metal layer to the gate and the source/drain regions and also connects two metal layers in the interconnects. The fabrication of a tungsten plug typically comprises the sequence of the deposition of premetal dielectric (PMD); patterning and etching of the contact hole; deposition of Ti and TiN films; and finally, deposition of W by chemical vapor deposition (CVD). The tungsten plug process is commonly used in sub-0.5- $\mu\text{m}$  CMOS process technologies, where it has been successfully implemented to provide aggressive contacted metal pitch. Increasing demands on the interconnect system to provide the maximum density possible at the technology nodes of 0.25  $\mu\text{m}$  and beyond require the overlaying metal pitch to be pushed to the limits of lithography. To achieve this in conjunction with low via resistance requires the metal-via overlap to be reduced to zero. Such an approach (called borderless contact), however, leads to unavoidable exposure of the tungsten plug due to misalignment and variation in the critical dimension of the vias and metal features.<sup>1,2</sup>

\* To whom correspondence should be addressed. Tel.: +886-6-275-7575, ext. 62695. Fax: +886-6-234-4496. E-mail: bhchen@alumni.rice.edu.

<sup>†</sup> National Cheng Kung University.

<sup>‡</sup> National University of Singapore.

<sup>§</sup> Chartered Semiconductor Manufacturing Ltd..

<sup>⊥</sup> Institute of Materials Research and Engineering.

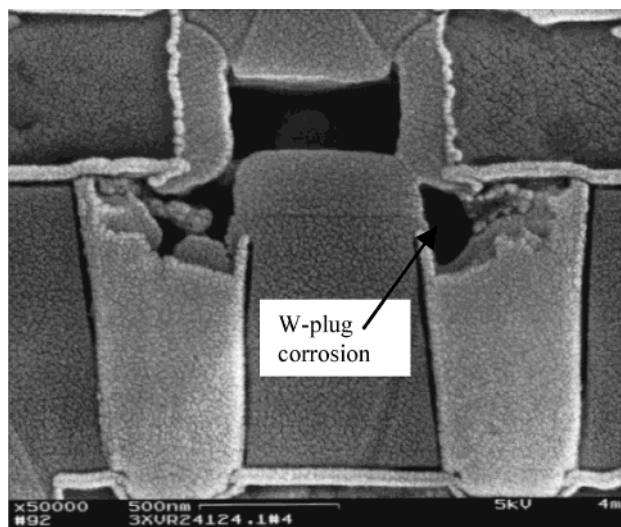


**Figure 1.** SEM micrograph showing the EOL (end-of-the-line) of a via chain cleaned in EKC265 solution during post-metal etch strip.

As the etch processes of the metal or the polysilicon have progressed, the subsequent cleaning steps have been required to strip the photoresist and to remove the “sidewall polymer”, etc.<sup>3</sup> When the tungsten plugs were exposed to the hydroxylamine-based cleaning solutions commonly used as the resist strippers, corrosion of the tungsten plugs occurred during the wet-cleaning process.<sup>3,4</sup> Figure 1 shows the corrosion originating at the tungsten that has been exposed to the cleaning solution. The corroded tungsten plugs lead to the drastic increase in resistance and have become one of the key reliability issues for metal interconnects as the feature size shrinks

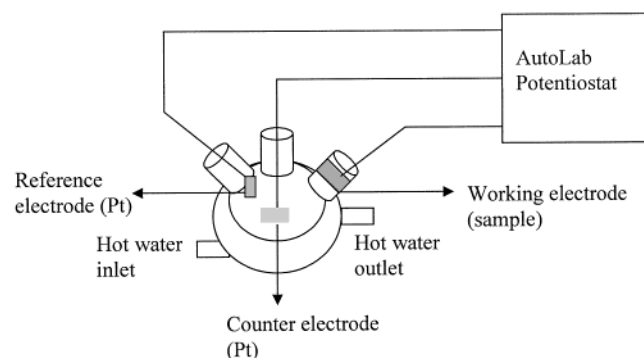
to 0.25  $\mu\text{m}$  and beyond, where the zero-overlap design rule is applied.<sup>1,5-7</sup>

Undoubtedly, knowledge of the electrochemical behavior of tungsten in various cleaning solutions is critical to solve this corrosion problem and to improve the device's reliability. The EKC265, which is a hydroxylamine-based semiaqueous alkaline solution (water content < 50%), is one of the widely used post-etching residue strippers in the semiconductor industry.<sup>8</sup> It is, thus, the purpose of this work to study and to investigate the corrosive behavior of tungsten in the EKC265-based electrolytes.

## 2. Experimental Method and Materials

Blanket tungsten wafers were provided by the Chartered Semiconductor Manufacturing (Singapore). A 1- $\mu\text{m}$  layer of  $\text{SiO}_2$  was first deposited using CVD on a 200-mm silicon wafer, followed by the deposition of a 20-nm Ti/TiN barrier layer. A tungsten film of 400-nm thickness was then deposited by CVD. The wafer was diced into smaller samples ( $1 \times 1 \text{ cm}^2$ ). Prior to solution treatment, the tungsten films were cleaned using reagent-grade deionized water (DI water, resistivity > 18  $\text{M}\Omega\cdot\text{cm}$ ), and dried under a  $\text{N}_2$  stream. DI water and diluted HCl (0.1 M) were used as additives to the EKC265 so that the effect of chloride ion and DI water on tungsten corrosion was investigated. The EKC265 was kindly donated by EKC Technology, Inc. (Hayward, CA). The main compositions in the EKC265 include the hydroxylamine, the alkanolamine and the 1,2-dihydroxybenzene as a chelating agent.<sup>9</sup> It is worth mentioning that 1,2-dihydroxybenzene has been widely used as an effective corrosion inhibitor in post-etch residue strippers.<sup>10,11</sup>

The tungsten films were electrochemically treated in four EKC265-based electrolytes: (i) pure EKC265, (ii) EKC265/HCl (8:1 by volume), (iii) EKC265/DI water (1:1 by volume), and (iv) EKC265/DI water/HCl (4:4:1 by volume). It has to be mentioned that the pH values of these four electrolytes do not differ much and are close to 12. Tafel extrapolation and potentiometry measurement (the open-circuit potential  $E_{\text{corr}}$  vs time) on tungsten films were performed on the AutoLab potentiostat/galvanostat equipped with AutoLab software (AutoLab, Netherlands). All the electrochemical measurements were carried out in a Faraday cage.



A house-made glass corrosion cell, schematically shown above, with three separate necks for reference, counter, and working electrodes and the inlet/outlet for circulating hot water for temperature control, was used. Stoppers made of Teflon were used on each neck. The sliced tungsten sample was fitted onto a Teflon holder

and held tightly between the O-rings, leaving a surface area of 0.283  $\text{cm}^2$  exposed to the electrolytes. Note that the platinum electrode was employed as the reference electrode, in addition to the use as the counter electrode, owing to the size limitation in the sample and the corrosion cell.

Following these solution treatments, the tungsten films were dried by pure nitrogen and sent for further surface analysis by SEM, AFM, and XPS. The physical conditions of the tungsten surface were evaluated using a JEOL-5600 field emission scanning electron microscope (FESEM). The surface morphologies of the tungsten films before and after solution treatments were characterized using a Dimension 5000 atomic force microscopy (Digital Instruments, Santa Barbara, CA) instrument. The root-mean-square (RMS) surface roughness was obtained by scanning the samples over a  $5 \times 5 \mu\text{m}^2$  area.

The XPS measurements were performed using an AXIS Hsi spectrometer (Kratos Analytical Ltd., England) equipped with a monochromatic Al X-ray source ( $K\alpha$ , 1486.6 eV) at a constant dwelling time of 100 ms and a pass energy of 40 eV. The measurements were taken with the charge neutralizer on. The pressure in the analysis chamber was maintained at  $5.0 \times 10^{-8}$  Torr or lower during the measurement. High-resolution core-level spectra were collected from the tungsten 4f, the oxygen 1s, and the carbon 1s regions. Integrated intensities of these regions were normalized using the published sensitivity factors to calculate the percent atomic concentrations of the surface region. Curve fittings were carried out on the tungsten and oxygen spectra using XPSpeak 4.1 so that individual peaks could be identified and the oxidation states of the tungsten surface could be recognized using the published spectra data.<sup>12,13</sup>

## 3. Results

**3.1 Tafel Plots and the Open-Circuit Potential Results.** The first set of electrochemical experiments was carried out at ambient temperature ( $\sim 23^\circ\text{C}$ ) and consisted of measuring the corrosion-current densities ( $I_{\text{corr}}$ ) and the charge-transfer resistance ( $R_{\text{ct}}$ ) from Tafel curves and Tafel extrapolation.<sup>14,15</sup> It is of note that  $R_{\text{ct}}$  can be experimentally obtained if the system under investigation follows the Tafel behavior.<sup>14,15</sup> Figure 2 shows the Tafel curves obtained at room temperature for the tungsten films exposed to the pure EKC265 solution and the electrolytes of the EKC265 incorporated with deionized water or 0.1 M HCl, as well as both deionized water and 0.1M HCl, respectively. As previously mentioned, owing to the size limitation of the corrosion cell, another Pt electrode was employed as the reference electrode, in addition to the Pt counter electrode. Hence, the corrosion potentials reported in this work are all referred to the Pt reference electrode. Table 1 lists the corrosion-current densities and the open-circuit potential ( $E_{\text{corr}}$ ) determined by Tafel curves as well as the values of the charge-transfer resistance from the Tafel extrapolation. Table 1 also tabulated the corrosion rate expressed in penetration units, mil per year (mpy), based on Faraday's law.<sup>16</sup>

The experiments were repeated at  $65^\circ\text{C}$ , and the resulting Tafel curves are again displayed as Figure 3. The corrosion-current density, the open-circuit potential, and the charge-transfer resistance are again tabulated in Table 2. The corresponding corrosion-current densi-

**Table 1. Corrosion-Current Density ( $I_{\text{corr}}$ ), Open-Circuit Potential ( $E_{\text{corr}}$ ), Charge-Transfer Resistance ( $R_{\text{ct}}$ ), and Corrosion Rate of the Tungsten Films Tested in the EKC265-Based Electrolytes at Ambient Temperature<sup>a,b</sup>**

electrolyte	$I_{\text{corr}}$ ( $\mu\text{A}/\text{cm}^2$ )	$E_{\text{corr}}$ (V)	$R_{\text{ct}}$ ( $\text{k}\Omega$ )	corrosion rate (mpy)
EKC265	0.64	-0.09	90.0	0.0205
EKC265 + 0.1 M HCl (8:1 v/v)	0.77	-0.11	84.0	0.0245
EKC265 + DI water (1:1 v/v)	1.51	-0.10	16.5	0.0481
EKC265 + DI water + 0.1 M HCl (4:4:1 v/v)	3.95	-0.12	14.6	0.126

<sup>a</sup> ~23 °C. <sup>b</sup> 0.1 M HCl was used as the source of chloride ions in the electrolytes.

**Table 2. Corrosion-Current Density ( $I_{\text{corr}}$ ), Open-Circuit Potential ( $E_{\text{corr}}$ ), Charge-Transfer Resistance ( $R_{\text{ct}}$ ), and Corrosion Rate of the Tungsten Films Tested in the EKC265-Based Electrolytes at 65 °C<sup>a</sup>**

electrolytes	$I_{\text{corr}}$ ( $\mu\text{A}/\text{cm}^2$ )	$E_{\text{corr}}$ (V)	$R_{\text{ct}}$ ( $\text{k}\Omega$ )	corrosion rate (mpy)
EKC265	0.884	-0.08	78.8	0.0283
EKC265 + 0.1 M HCl (8:1 v/v)	3.42	-0.14	21.0	0.109
EKC265 + DI water (1:1 v/v)	4.53	-0.10	18.7	0.145
EKC265 + DI water + 0.1 M HCl (4:4:1 v/v)	4.83	-0.14	11.9	0.154

<sup>a</sup> 0.1 M HCl was used as the source of chloride ions in the electrolytes.

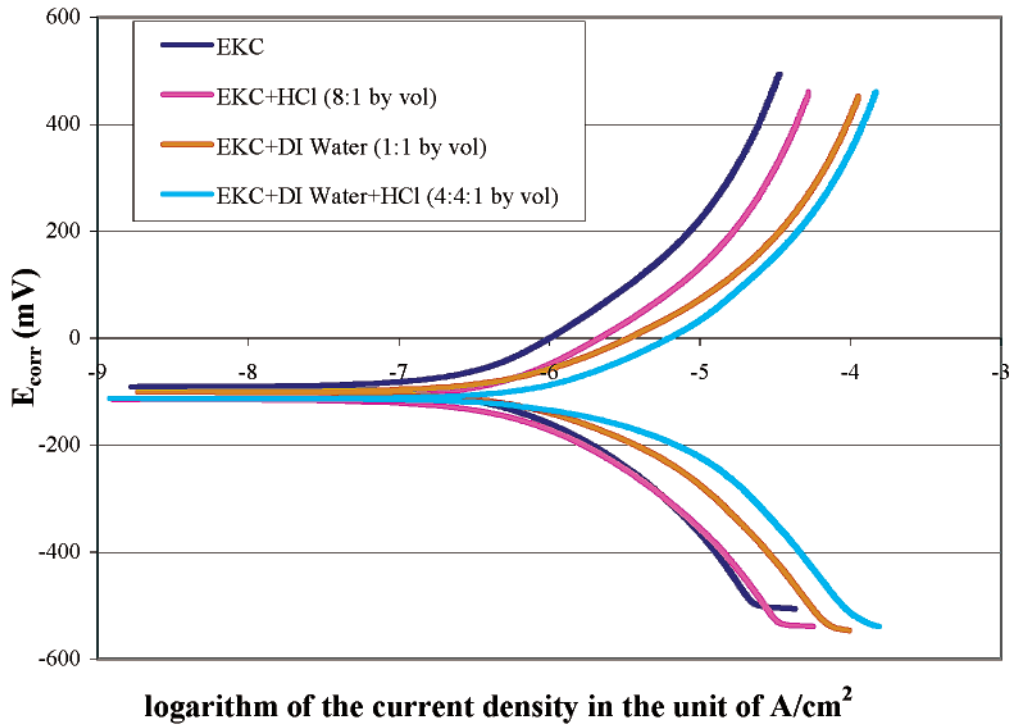


**Figure 2.** Tafel curves for CVD tungsten films in the absence or presence of DI water and  $\text{Cl}^-$  in EKC265 solutions at room temperature. Pt is used as the reference electrode.

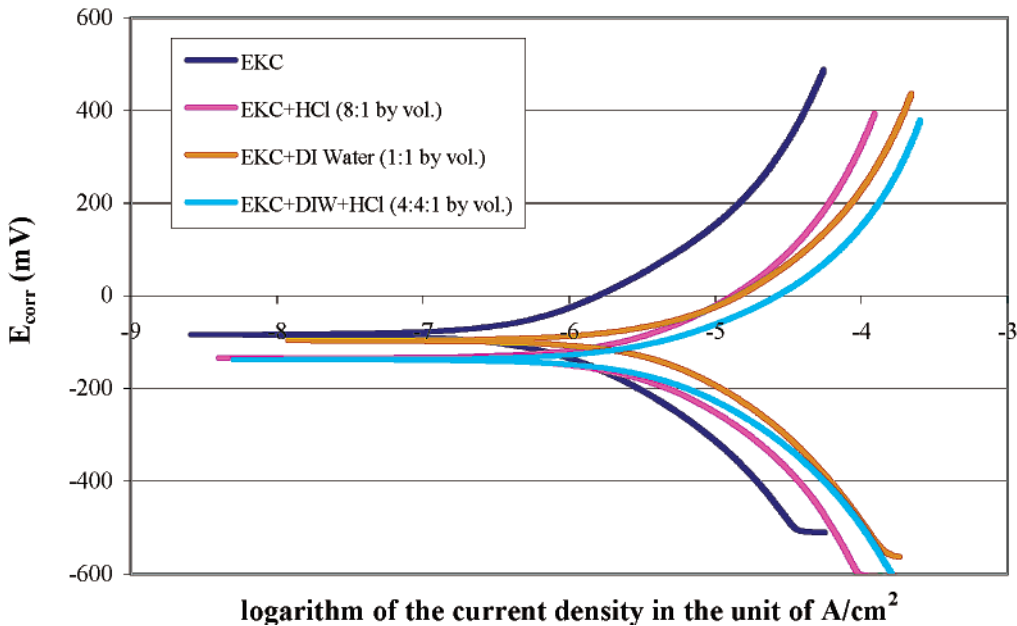


**Figure 3.** Tafel curves for CVD tungsten films in the absence or presence of DI water and  $\text{Cl}^-$  in EKC265 solutions at 65 °C. Pt is used as the reference electrode.



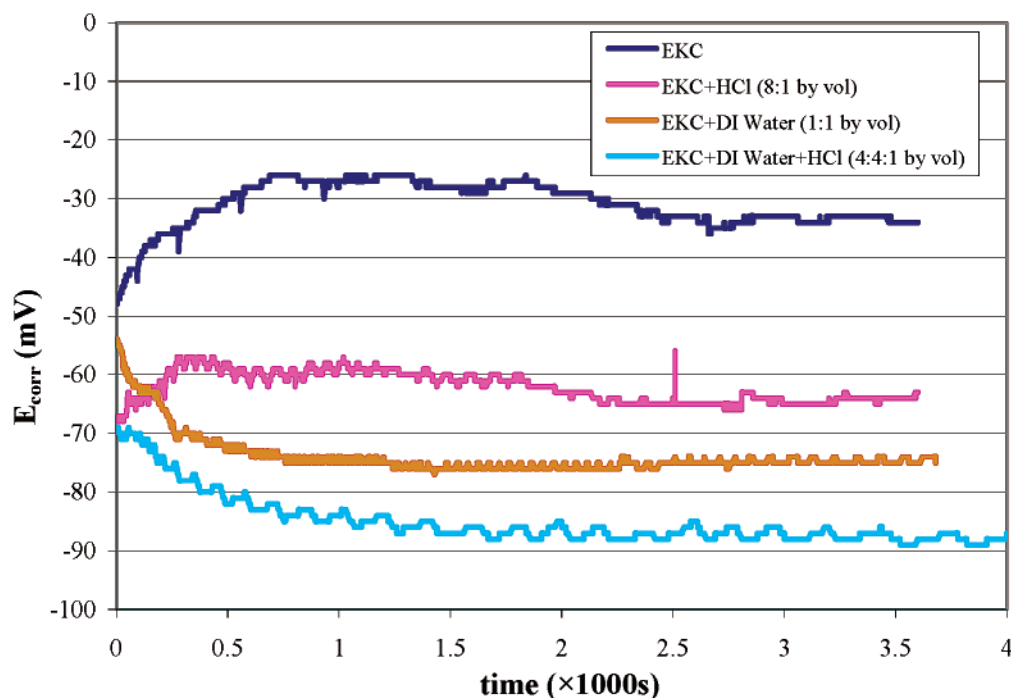


**Figure 4.** Potentiometry of tungsten in EKC265-based electrolytes at 65 °C. Pt is used as the reference electrode.

ties at 65 °C are relatively higher than those in the respective corrosive environments at ambient temperature in all four electrolytes. It is clear that the tungsten films suffer from the most severe corrosion in the EKC265 solutions with added deionized water and HCl at both temperatures. Interestingly, the corresponding corrosion rates of the tungsten are 1 order of magnitude higher than those in the pure EKC265 solutions at both temperatures.

The data of the open-circuit potential  $E_{\text{corr}}$  extrapolated from the Tafel curves do not take into account the fact that the  $E_{\text{corr}}$  varies with time as a result of the change of the surface states of the tungsten films after interacting with electrolytes. From the potentiometry ( $E_{\text{corr}}$  vs time) in the four electrolytes at 65 °C shown in the Figure 4, it can be seen that in the first two electrolytes, namely, the pure EKC265 solution and the EKC265 with HCl, the potential becomes less negative with time, suggesting that the tungsten surfaces were passivated in the solutions. On the contrary, the opposite trends in those for the EKC265 solutions with added DI water only, as well as both the DI water and HCl, suggests that the tungsten film was corroded faster. This was consistent with the high corrosion currents shown earlier in Table 2.

**3.2 XPS Results.** The resulting chemical composition of the tungsten surfaces after solution treatment in the four electrolytes was further investigated through identification of the peaks present in the tungsten 4f core level spectra using XPSPeak 4.1.<sup>12,13</sup> The spectra of the dissipated W 4f electrons collected from the as-received tungsten films and samples treated in the four electrolytes are shown in Figure 5. Significant changes in the W 4f spectrum for each sample were observed, which can be explained in terms of the alteration of surface chemical compositions. Table 3 shows the relative compositions of different oxidation states of tungsten after being treated in the four electrolytes. It can be seen from the table that more  $\text{WO}_2$  are formed than  $\text{WO}_3$  as DI water and chloride are added to the electrolytes. This

change of tungsten oxide composition is believed to be responsible for the increasing corrosion rate observed in those electrolytes.

**3.3 Surface Morphology and Roughness Measurements.** The surface morphology of the tungsten films was characterized by using the SEM for those with/without being treated in the electrolytes. Moreover, the quantitative measurements of the surface morphology are provided with the AFM operated in the tapping mode. The root-mean-squares (RMS) of the surface roughness of all the samples are tabulated in Table 4. Interestingly, the RMS roughness does not differ much.

Figure 6 shows the SEM micrograph of the tungsten film without any treatment. Likewise, Figure 7 exhibits the SEM micrographs of the tungsten films treated in the four different electrolytes at 65 °C. All the SEM pictures presented in Figures 6 and 7 were taken at a magnification of 30 000 times, and the white bar in the bottom represents 100 nm. The existence of grain structures on the as-received tungsten film (Figure 6) can be clearly observed. The grain size is of the order 100–1000 nm, and the RMS roughness is  $\sim 11.1$  nm. In contrast, the grain structures are not clearly observed when the bulky or the localized (pitting) corrosion occurs. Interestingly, the sample treated with the EKC265 only still retains the distinguishable grain structures. Coincidentally, it possesses the least corrosion current density and the least amount of  $\text{W}^{4+}$  among all the solution-treated samples. The pits of  $\sim 60$  nm in diameter are clearly observed as densely scattered in the Figure 7d, in which the electrolyte gives the highest corrosion rate but the least amount of  $\text{W}^{6+}$ .

#### 4. Discussion

The results presented in the preceding sections demonstrate how the electrochemical response of the tungsten in the EKC265 solution has been impacted by the presence of DI water and  $\text{Cl}^-$  by comparing the corrosion-current density, the open-circuit potentials, and the

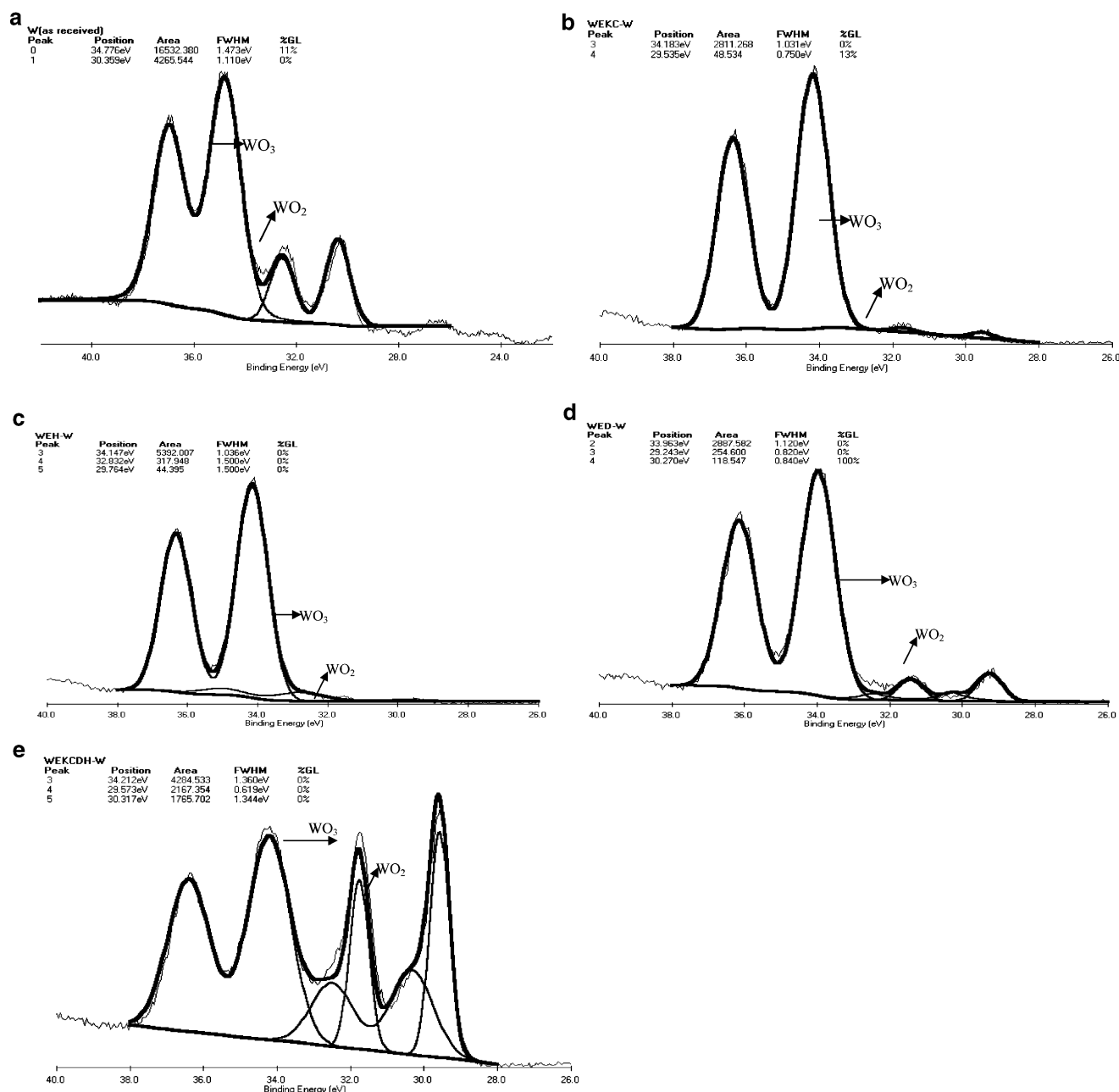


**Figure 5.** XPS Spectra of tungsten after treated in different electrolytes: (a) as received, (b) treated in EKC265, (c) treated in EKC265 + HCl (8:1 v/v), (d) treated in EKC265 + DI water (1:1 v/v), and (e) treated in EKC265 + DI water + HCl (4:4:1 v/v).

**Table 3.** Atomic Composition of the Tungsten in Different Oxidation States after Treatment in the EKC265-based Electrolytes at 65 °C<sup>a</sup>

sample	W <sup>0</sup> (at. %)	W <sup>4+</sup> (at. %)	W <sup>6+</sup> (at. %)
as received	20.4	—	79.5
EKC265	—	1	99
EKC265 + 0.1 M HCl (8:1 v/v)	0.78	5.52	93.7
EKC265 + DI water (1:1 v/v)	3.59	7.81	88.6
EKC265 + DI water + 0.1 M HCl (4:4:1 v/v)	21.5	26.4	52.1

<sup>a</sup> 0.1 M HCl was used as the source of chloride ions in the electrolytes.

charge-transfer resistances. It is worth mentioning that addition of chloride ion to the electrolyte is to simulate the presence of the Cl contaminants incurred from the previous dry-etching procedure involving the Cl<sub>2</sub>-containing plasmas.

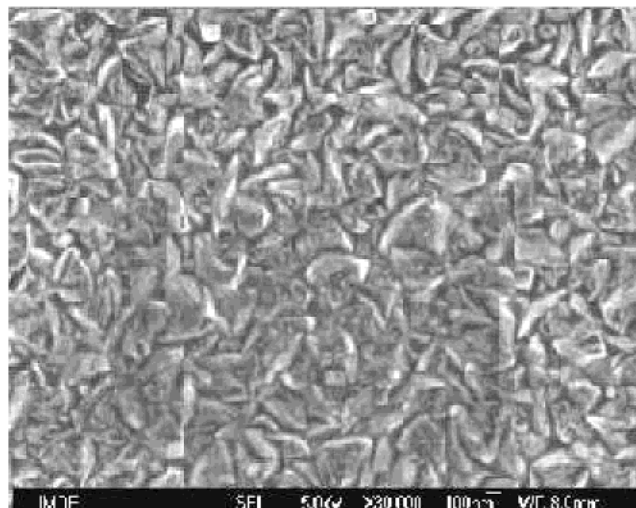
The first set of data obtained at room temperature shows that the corrosion-current density is <1 μA/cm<sup>2</sup> in the pure EKC265 solution, which is acceptable for

corrosion prevention. It is well-known that tungsten is susceptible to electrochemical corrosion in basic environments.<sup>17–19</sup> The corrosion resistance of the tungsten decreases with increasing pH value. Interestingly, the pH value of the EKC265 solution is ~12, which is considered to be highly basic. This high pH value is good for the removal of the organic residues formed during the metal etching process,<sup>3</sup> but not for preventing the

**Table 4. Root-Mean-Square (RMS) of the Surface Roughness of the Tungsten Films before and after Being Treated in the Different Electrolytes at 65 °C<sup>a</sup>**

conditions	RMS roughness (nm)
as received	11.11
EKC265	10.7
EKC265 + 0.1 M HCl (8:1 v/v)	10.4
EKC265 + DI water (1:1 v/v)	13.9
EKC265 + DI water + 0.1 M HCl (4:4:1 v/v)	11.3

<sup>a</sup> 0.1 M HCl was used as the source of chloride ions in the electrolytes.

**Figure 6.** SEM micrograph of the top surface of a CVD tungsten film taken at a magnification of 30 000 $\times$ .

tungsten corrosion.<sup>20</sup> The absence of the severe tungsten corrosion, evidently observed from the low corrosion-current density, in the pure EKC265 solution is due to the presence of the corrosion inhibitors, 1,2-dihydroxybenzene and derivatives, in the solution, as reported by the manufacturer. Nevertheless, the effectiveness of the corrosion inhibitors in the EKC265 solution will be largely decreased by increasing temperature or by the presence of certain substances that are able to contribute to the tungsten corrosion mechanism.

In practice, EKC265 is commonly used for post-etch cleaning between 60 and 80 °C. The results obtained at 65 °C show that the corrosion-current density is significantly higher than that at ambient condition. It is also observed that the addition of DI water, Cl<sup>-</sup> ions, or both DI water and Cl<sup>-</sup> ions to the EKC265 solution increases the corrosion-current density and shifts the open-circuit potential to more negative values at both room temperature and 65 °C. The lower charge-transfer resistances (Table 2) demonstrate that the addition of DI water or Cl<sup>-</sup> improves the ability of the electrolytes to carry electrons and ions from and to the metal surface and, thus, enhances the corrosion reactions. Such a synergistic effect of DI water and Cl<sup>-</sup> ion becomes more significant at 65 °C (Tables 1 and 2). The worst situation takes place when both DI water and Cl<sup>-</sup> are present in the EKC265 solution, as the highest corrosion-current density is observed. Unfortunately, this often happens during the post-etch cleaning process when DI water is introduced in such a wet cleaning process, and there are always Cl<sup>-</sup> ions, even trace amounts only, present on the side wall of the feature after the Cl<sub>2</sub>-containing plasma etch.

The open-circuit potential ( $E_{\text{corr}}$ ) is important in evaluating corrosion behavior, since it reflects the driving force of the corrosion reaction. The more negative the  $E_{\text{corr}}$  is, the more prone the metal is toward corrosion in the solutions. It can be observed that the  $E_{\text{corr}}$  is a strong function of time in the early stage (Figure 4), which indicates that the oxide states of the tungsten change significantly as a result of the W dissolution or the pitting formation. In the experiments, the  $E_{\text{corr}}$  becomes more negative in the EKC265 solution with the presence of Cl<sup>-</sup> or DI water. Hence, it is confirmed again that the tungsten is more inclined to corrosion when DI water, Cl<sup>-</sup> ions, or both are present, which is consistent with the previous data on the corrosion-current density.

Although both DI water and Cl<sup>-</sup> can enhance the corrosion of tungsten, they function differently. The dissolution and passivation mechanisms of the tungsten films in aqueous solutions at different pH values, as well as the formation and dissolution of tungsten oxides, have been extensively studied.<sup>17–21</sup> The corrosion resistance of tungsten is largely dependent on the stability of the tungsten oxides. In the absence of an oxidizer, the tungsten surface is passivated most effectively at acidic solutions.<sup>19</sup> A duplex oxide layer containing WO<sub>2</sub> and WO<sub>3</sub> is formed at low pH. The WO<sub>2</sub> is a metallic conductor, while the WO<sub>3</sub> is only an ionic conductor. Stein et al.<sup>19</sup> drew their conclusion that the passivation of the tungsten surface is primarily dictated by the formation of the WO<sub>3</sub>.

Among the oxides of tungsten, the hexavalent tungsten derivatives are the most stable.<sup>20</sup> Furthermore and likewise, Astha et al.<sup>20</sup> concluded that tungsten in the 6+ oxidation state has been found to play an important role in the passivation behavior of the tungsten.<sup>20</sup> However, the formation rate of the WO<sub>3</sub> layer decreases with increasing temperature and pH values.<sup>17</sup> In alkaline solutions (pH > 8), the WO<sub>3</sub> will be rapidly dissolved.<sup>19</sup>

The XPS spectra collected from the tungsten samples clearly demonstrate how the atomic compositions of the surface tungsten oxides change in these different electrolytes. Table 3 indicates that the elemental tungsten (W<sup>0</sup>) of the as-received tungsten samples is mostly oxidized to WO<sub>3</sub> by the EKC265 solution, even though its pH value is  $\sim$ 12. Apparently, the corrosion inhibitors in the EKC265 electrolytes could effectively prevent the extensive dissolution of the WO<sub>3</sub> and, thus, protect the underlying tungsten.

The low corrosion-current density in the pure EKC265 solution (Table 1) demonstrates the effectiveness of this protective oxide layer in corrosion resistance. The addition of DI water or chloride ions, however, degrades the function of the corrosion inhibitors and alters the composition of the oxides formed on the tungsten films. A duplex oxide layer, which contains WO<sub>2</sub> and WO<sub>3</sub>, was formed instead of the stable WO<sub>3</sub> oxide layer, as evidenced by the increasing concentration of WO<sub>2</sub> in Table 3.

An increase in the WO<sub>2</sub> amount in the WO<sub>2</sub>/WO<sub>3</sub> duplex layer leads to a reduction in corrosion resistance. For example, the highest atomic ratio of WO<sub>2</sub> to WO<sub>3</sub> is found in the EKC265 solution with both DI water and Cl<sup>-</sup> ions added, whereas the corrosion-current density is also the highest in this electrolyte. Tafel data and XPS analysis indicate that addition of DI water and Cl<sup>-</sup> results in a significant shift from a WO<sub>3</sub> layer to a WO<sub>2</sub>/



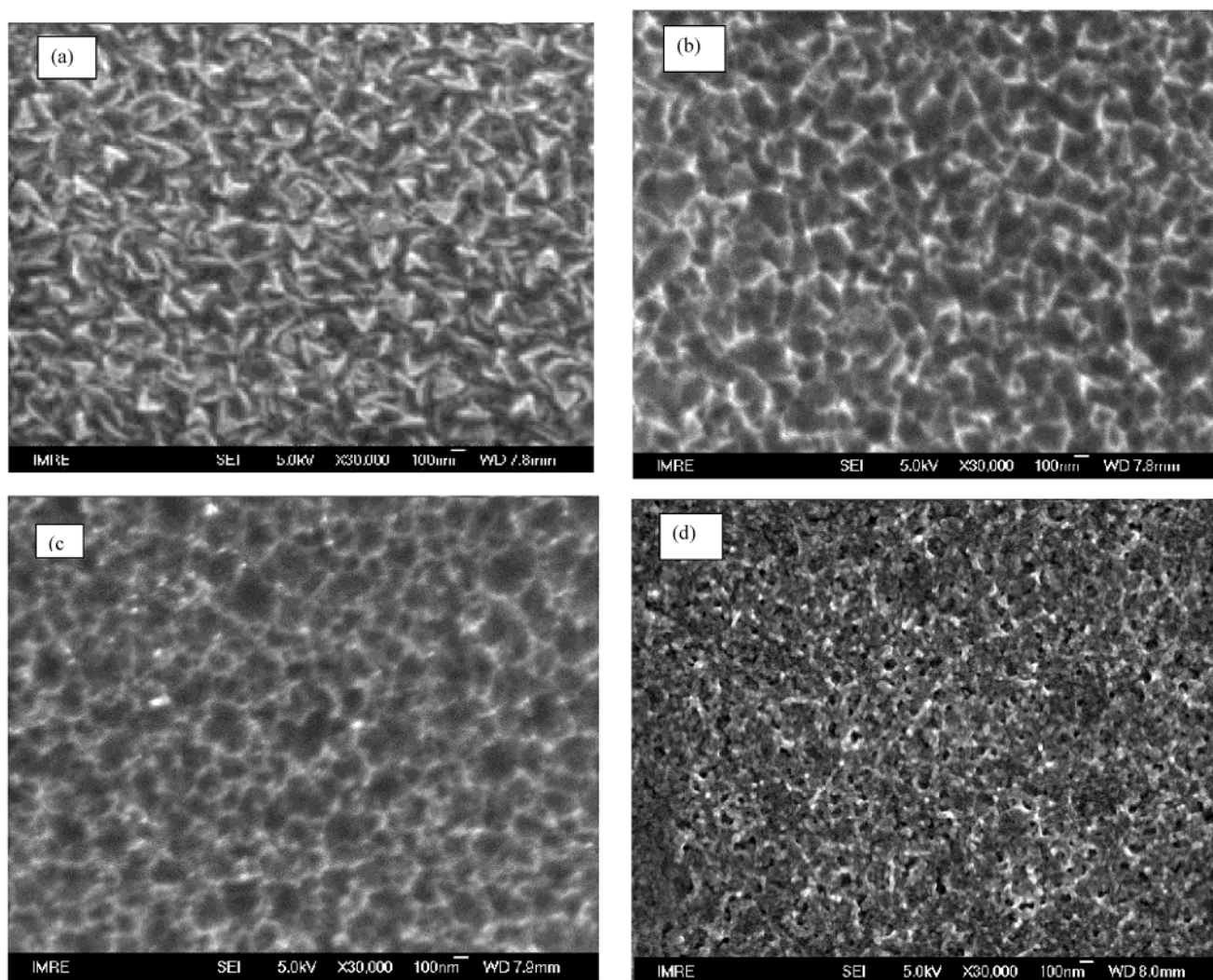


**Figure 7.** SEM micrographs of tungsten surface after being treated in different electrolytes at 65 °C: (a) treated in EKC265, (b) treated in EKC265 + HCl (8:1 v/v), (c) treated in EKC265 + DI water (1:1 v/v), and (d) treated in EKC265 + DI water + HCl (4:4:1 v/v).

WO<sub>3</sub> duplex layer on the tungsten surface, thus making the tungsten less resistant to electrochemical attack.

The chloride ions play particularly a very important role in the corrosion of the tungsten. For example, Di Quarto et al.<sup>21</sup> found that the Cl<sup>-</sup> ions could particularly assist the pitting formation of the tungsten by forming the intermediate product WO<sub>2</sub>Cl<sub>2</sub>. Such pitting phenomena could be observed in the SEM micrograph (Figure 7d). Additionally, the dissolution mechanism of the WO<sub>3</sub> films in chloride is of the first order.<sup>17</sup> That is, the dissolution rate will increase linearly with the chloride concentration.

SEM micrographs show the surface morphology of tungsten films after electrochemical treatments. They also provide the visual evidence of tungsten loss arising from either bulky removal or localized removal (pitting corrosion). When compared with the surface morphology of the as-received tungsten films (Figure 6), Figure 7a and b does not show a very distinct difference, and the grains can be clearly seen. This suggests that tungsten films have not suffered from significant attack by these two electrolytes yet. Instead, the AFM images suggest that the surface roughnesses are slightly reduced in these two electrolytes. This may be primarily due to the removal of the surface oxides by the alkaline electrolytes. These observations are consistent with the previ-

ous Tafel data, since the corrosion-current densities are relatively low in these two electrolytes.

However, in Figure 7c, noticeable distortion of the grain structures is observed, which indicates that the tungsten has been eroded to certain extent. After treatment in EKC265 with DI water and Cl<sup>-</sup>, tungsten has been drastically corroded, and the attack is highly nonuniform so that the grain structure has been totally destroyed and corrosion pits appear (Figure 7d). Both bulky and localized tungsten losses occur in this case. That is why the corrosion-current density is the highest and the potential is the most negative. As aforementioned, the chloride ions could enhance the pitting corrosion of the tungsten.<sup>21</sup>

Finally, the highly alkaline solutions among the commercially available cleaning solutions may seem unattractive, since WO<sub>3</sub> tends to be rapidly dissolved. In contrast, the high pH environment is favorable for removing organic residues formed during the metal etching. Therefore, a compromise has to be reached. This may include (1) finding a better corrosion inhibitor as the additive to the cleaning solution and (2) employing a more effective method to remove the residue Cl<sup>-</sup>. To achieve that, a better understanding of the functions of individual components in the cleaning solution and the interaction between Cl<sup>-</sup> and those components is



necessary, as well as knowledge of transformation among different oxidation states of tungsten.

## Conclusion

The electrochemical behavior of tungsten in the EKC265 solutions with added chloride ions, DI water, or both was investigated to elucidate the effect of  $\text{Cl}^-$  and DI water on tungsten corrosion in the post-etch cleaning solution. The electrochemical data from the Tafel extrapolation and the potentiometry in various electrolytes at different temperatures were correlated with the data from X-ray photoelectron spectroscopy (XPS) and scanning electron microscopy (SEM). Results showed that the presence of  $\text{Cl}^-$  and DI water increased the corrosion-current density and shifted the open-circuit potential to more negative values, indicating the synergistic effect of DI water and  $\text{Cl}^-$  on the tungsten corrosion. The XPS spectra collected from tungsten samples treated in the electrolytes clearly demonstrated the shift of the oxidation states of tungsten from  $\text{WO}_3$  to a nonprotective  $\text{WO}_2/\text{WO}_3$  duplex film as a result of the presence of additives, which made tungsten more prone to attack by the electrolytes. SEM micrographs showed that both bulky and pitting corrosion occurred when tungsten was attacked by the electrolyte containing DI water and  $\text{Cl}^-$ . In industrial post-etch cleaning, it is highly possible that trace amounts of  $\text{Cl}^-$  may remain in the metal structure when the cleaning solution and DI water are introduced to the structure to remove the residues after the metal etching process. As a result, severe corrosion has been reported.

## Acknowledgment

The authors are grateful to the National University of Singapore and the Chartered Semiconductor Manufacturing (Singapore) as well as the Economy Development Board of the Republic of Singapore for financial support. The authors would further thank Ms. Sammatha Fam and Mr. Sian Khong Tan for their help in the XPS measurements and analysis as well as the EKC Technology, Inc. (Hayward, California) for the chemical samples.

## Literature Cited

- (1) Bothra, S.; Sur, H.; Liang, V. A New Failure Mechanism by Corrosion of Tungsten in a Tungsten Plug Process. *Microelectron. Reliab.* **1999**, *39*, 59.
- (2) Small, R. J.; Peterson, M. L.; Gorman, A. M. Post Clean Treatment and Post CMP Solutions for Metal and Particle Removal from VLSI Structures. *SEMICON China 98 Technical Symposium*, 1998.
- (3) Kirk, S. J.; Small, R. The Effect of DI Water and Intermediate Rinse Solutions on Past Metal Etch Residue Removal Using Semi-Aqueous Cleaning Chemistries. *Solid State Phenom.* **2001**, *76–77*, 307.
- (4) Koh, L.-T.; Chooi, S. Y. M.; Chok, K.-L.; Li, H.-M.; Ng, F.-H. A Study on the Effect of Post Metal Etching Polymer Strip Process on Via Resistance. *Mater. Res. Soc. Symp. Proc.* **1999**, *564*, 451.
- (5) Chooi, S. Y. M.; Ismail, Z.; Ee, P. Y.; Zhou, M. S. Post-Etching Polymer Removal in Sub-Half-Micron Device Technology. *Proc. of SPIE* **1998**, *3508*, 181.
- (6) Bothra, S.; Pramanik, D.; Weiling, M.; Gabriel, C.; Sur, H.; Lin, X. W. W-Plug Via Integration Issues. *Solid State Technol.* **1997**, *40*, 77.
- (7) Obeng, Y. S.; Kang, S. H.; Huang, J. S.; Oates, A. S.; Lin, X. Impact of Post Via-Etch Cleans on Mechanical Reliability of W-Plug Vias. *Thin Solid Films* **2001**, *391*, 149.
- (8) Lanckmans, F.; Baklanov, M.; Alaerts, C.; Vanhaelemeersch, S.; Maex, K. Post Dry-Etch Cleaning Issues of an Organic Low-K Dielectric. *Solid State Phenom.* **1999**, *65–66*, 89.
- (9) Lee, W. M. Cleaning compositions for removing etching residue and method of using. U.S. Patent 6,000,411, 1999.
- (10) Ash, M.; Ash, I. *Handbook of Corrosion Inhibitors*; Synapse Information Resources Inc: New York, 2000.
- (11) Peters, L. J. Strippers No More: Aqueous Approaches to Residue Removal. *Semicond. Int.* **1999**, *22* (12), 84.
- (12) Perry, S. S.; Galloway, H. C.; Cao, P.; Mitchell, E. J. R.; Koeck, D. C.; Smith, C. L.; Lim, M. S. The Influence of Chemical Treatments on Tungsten Films Found in Integrated Circuits. *Appl. Surf. Sci.* **2001**, *180*, 6.
- (13) Sarma, D. D.; Rao, C. N. R. XPES Studies of Oxides of Second- and Third-row Transition Metals Including Rare Earths. *J. Electron. Spectrosc. Relat. Phenom.* **1980**, *20*, 25.
- (14) Bard, A. J.; Faulkner, L. R. *Electrochemical Methods: Fundamentals and Applications*, 2nd ed.; John Wiley & Sons: New York, 2001.
- (15) Jones, D. A. *Principles and Prevention of Corrosion*, 2nd ed.; Prentice Hall: Upper Saddle River, NJ, 1996.
- (16) Fontana, M. G. *Corrosion Engineering*, 3rd ed.; McGraw-Hill: New York, 1987.
- (17) Mogoda, A. S.; Hefny, M. M.; El-Mahdy, G. A. Anodic Oxide Films on Tungsten: Formation and Dissolution in Acetic Solutions. *Corrosion* **1990**, *46*, 210.
- (18) Kneer, E. A.; Raghunath, C.; Raghavan, S.; Jeon, J. S. Electrochemistry of Chemical Vapor Deposition Tungsten Films with Relevance to Chemical Mechanical Polishing. *J. Electrochem. Soc.* **1996**, *143*, 4095.
- (19) Stein, D. J.; Hetherington, D.; Guilinger, T.; Cecchi, J. L. In Situ Electrochemical Investigation of Tungsten Electrochemical Behavior during Chemical Mechanical Polishing. *J. Electrochem. Soc.* **1998**, *145*, 3190.
- (20) Astha, S.; Balasubramaniam, R.; Parani, A. On the passivation of iron aluminides by addition of tungsten. *J. Mat. Sci. Lett.* **1999**, *18*, 1555.
- (21) Di Quarto, F.; Piazza, S.; Sunseri, C. Electrical Breakdown and Pitting in Anodic Films on Tungsten in Halogen Ion-Containing Solutions. *J. Electroanal. Chem.* **1988**, *248*, 117.

Received for review January 13, 2003

Revised manuscript received August 4, 2003

Accepted August 9, 2003

IE030025H